Soft Matter



Cite this: *Soft Matter*, 2011, **7**, 2762

www.rsc.org/softmatter

**PAPER**

# Controllable self-assembled laminated nanoribbons from dipeptide-amphiphile bearing azobenzene moiety†

**Yiyang Lin,[a] Yan Qiao,[a] Peifeng Tang,[a] Zhibo Li[b] and Jianbin Huang*[a]**

***Received 23rd September 2010, Accepted 27th November 2010***
**DOI: 10.1039/c0sm01050b**



Artificial peptide self-assembly is an appealing research subject which has been demonstrated to be a reliable approach to create hierarchical nanostructures and biomaterials. In this paper, a dipeptide-amphiphile incorporated with an azobenzene moiety is synthesized, which are found to self-assemble into well-defined laminated nanoribbons as well as macroscopic hydrogel. The nanoribbons are formed by nanofibers aligning in nearly lamellar arrays. The driving force of dipeptide self-assembly is proposed to be a synergic effect of hydrophobic interaction, aromatic packing, and hydrogen bond. The addition of NaCl is found to promote hydrogelation and nanoribbon formation. Finally photoisomerization of the azobenzene group is utilized to rationally control dipeptide self-assembly and hydrogel formation by remote light input.

## Introduction

Many natural biomolecules (proteins, lipids, and DNA) can self-assemble into functional materials displaying a hierarchy of structure over several length scales.[1] In particular, structural protein-based hydrogels are used for many applications, ranging from cosmetic thickeners to drug delivery and tissue engineering.[2] These materials are usually extracted from natural sources, which may give rise to inconsistent properties unsuitable for biomedical applications. Artificial peptides, which are employed as the building blocks of proteins, begin to allow the incorporation of the structures and functions of proteins into synthetic materials.[3] These peptide materials are particularly desirable for control over nanoscale ordering through self-assembly in the field of nanotechnology and biotechnology with the increased capability to respond to living systems for tissue engineering and therapeutic delivery.[4]

Recently low molecular peptide-derivatives have attracted considerable attention because of their facile synthesis, variability of amino acid sequence, and ease of functionalization.[5] For example, Stupp has reported pH-induced self-assembly of a peptide-amphiphile to make nanostructured fibrous scaffold reminiscent of extracellular matrix. The cross-linked fibers are able to direct mineralization of hydroxyapatite to form a composite material in which the crystallographic *c* axes of hydroxyapatite are aligned with the long axes of the fibers.[6] A systematic study on single tail peptide-amphiphiles was conducted by the same group.[7] Hartgerink and co-workers have focused on the research of polypeptides without a hydrocarbon chain in aqueous solution.[8] Shimizu has synthesized dipeptide bolaamphiphiles which can self-assemble into vesicle-encapsulated microtubes.[9] It can be found that peptide derivatives preferentially self-organize into one-dimensional nanostructures such as fibers, tubes, ribbons, *etc*, which offer many potential applications in electronically and biologically active materials.[10]

Inspiration by these works has led us to synthesize novel dipeptide-amphiphiles bearing a glycylglycine group, and focus on the study of controllable supramolecular self-assembly. For the consideration of further bio-functional application, the research is conducted in aqueous solutions rather than organic solvents. Moreover, an azobenzene group was attached to the dipeptide-amphiphile to give light-activity. Light is expected to be an advantageous and important tool to change molecular structure as well as to manipulate amphiphile self-assemblies at different hierarchical levels.[11] This is because light can be operated in a clean environment free of any additional reagent. Another advantage of light over electric or ultrasound is that, light can be directed at a precise spatial location. In our study, hydrophobic hydrocarbon chains are also incorporated to the amphiphile skeleton to promote molecular self-assembly in water.

Combined with different techniques, the self-assembly behavior of dipeptide-amphiphiles in aqueous solution is investigated, which are demonstrated to spontaneously aggregate into well-defined nanoribbons at low concentrations. The formation and overlap of nanoribbons can further result into water gelation. From the results of FT-IR and CD spectrum, the molecular

[a]*Beijing National Laboratory for Molecular Sciences (BNLMS), State Key Laboratory for Structural Chemistry of Unstable and Stable Species, College of Chemistry, Peking University, Beijing, 100871, People's Republic of China. E-mail: JBHuang@pku.edu.cn; Fax: +86-10-62751708; Tel: +86-10-62753557*
[b]*CAS Key Laboratory of Photochemistry, Institute of Chemistry, Chinese Academy of Sciences, Beijing, 100080, People's Republic of China*

† Electronic supplementary information (ESI) available: Fluorescence intensity curve, gelation temperature, dynamic rheology, and additional TEM images. See DOI: 10.1039/c0sm01050b

origin of 1D nanostructure formation is proposed. The effect of salt addition and azobenzene photoisomerization on dipeptide-amphiphile self-assembly is also investigated. It is hopeful that this study can help to understand the mechanism of peptide-amphiphile self-assembly and will thereby help to design functional peptides materials.

## Experimental section

### Materials

4-Butylaniline and 4-hexylaniline were purchased from Alfa Aesar. Ethyl bromoacetate, glycylglycine, sodium nitrite, potassium hydroxide, hydrochloric acid (37%), and sodium hydroxide were bought from Beijing Chemical Reagents Company. All chemicals were used as received without further purification. The Millipore Milli-Q deionized water (18.2 MΩ/cm resistivity) was used for producing aqueous solution.

### Amphiphile synthesis

The synthesis of dipeptide-amphiphile is according to the following and outlined in Scheme 1.

(1) Compound 1:[12] 14.9 g *p*-butylaniline was dissolved in 200 mL water and 25 mL concentrated hydrochloric acid. The solution was cooled to 5 °C in an ice bath and reacted with 15 mL of aqueous sodium nitrite (6.67 M) at 5 °C for 1 h. The resulting diazonium solution was then coupled a solution containing 9.4 g phenol, 4 g sodium hydroxide, 10 g sodium carbonate, and 100 mL water at 0 °C for 2 h. The product was collected by filtration, dried in vacuum, and purified by recrystallization in hexane.

(2) Compound 2:[13] compound 1 (5.1 g, 20 mmol), ethyl bromoacetate (30 mmol), and potassium hydroxide (1.12 g, 20 mmol) was added to a round-bottomed flask containing 200 mL ethanol. The mixture was refluxed for 4 h and cooled in an ice bath. The solid product was collected by filtration and dissolved in 30 mL of water–methanol (10/90) and to the solution were added sodium hydroxide pellets. The mixture was heated to reflux for 30 min and a yellow solid formed. The compound 2 was obtained by collecting the solid and recrystallized from chloroform containing 2% glacial acetic acid.

(3) The compound 2 (1.63 g, 5 mmol) was added into a round-bottomed flask containing excessive thionyl chloride. The mixture was refluxed for 8 h and the resulting mixture was distilled under reduced pressure to remove most of the thionyl chloride. The product was added to a solution (20 mL) containing 15 mmol glycylglycine and 5 mmol sodium hydroxide

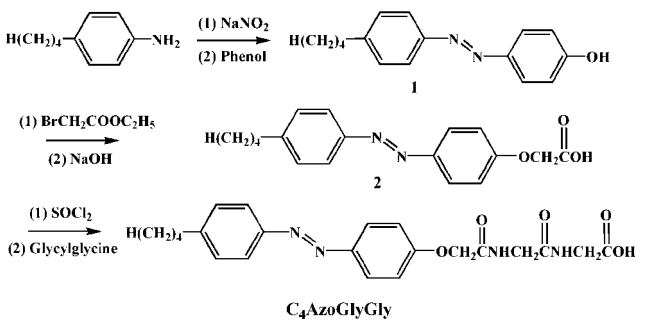


**Scheme 1** Organic synthesis of dipeptide-amphiphile $C_4$AzoGlyGly.

at 0 °C. The aqueous phase was acidified at room temperature to pH 2 with aqueous HCl. The solid was isolated by filtration and dissolved in hot alkaline solution. To this solution, aqueous HCl was slowly added and the precipitates were collected and dried in vacuum. $^1$H NMR (400 MHz, DMSO): 0.87 (t, 3H), 1.02 (m, 2H), 1.30 (m, 2H), 1.66 (t, 2H), 3.79 (s, 2H), 3.80 (s, 2H), 4.63 (s, 2H) 7.13 (d, 2H), 7.36 (d, 2H), 7.73 (d, 2H), 7.83 (d, 2H), 8.20 (m, 1H), 8.41 (m, 1H). Elemental analysis calcd (%) for $C_{22}H_{26}N_4O_5$: C 61.96, H 6.15, N 13.14; found: C 61.23, H 6.14, N 12.70.

### Sample preparation

The $C_4$AzoGlyGly solution mentioned in this paper is prepared by adding the desired amount of $C_4$AzoGlyGly solid into equal amount of sodium hydroxide solution and heated under stirring till completely soluble (~80 °C). The sample is then slowly cooled to room temperature. The gel–sol transition temperature ($T_{gel}$) was determined by the test-tube inversion method.

### Rheological measurement

The rheology was measured with a ThermoHaake RS300 rheometer. A cone-plate sensor was used with a diameter of 35 mm and a cone angle of 2°. A sample cover provided with the instrument was used to minimize the change in sample composition by evaporation during the measurement. Frequency sweep measurements were performed in the linear viscoelastic regime determined previously by dynamic stress sweep measurements.

### Negative-staining transmission electron microscopy

TEM micrographs were obtained with a JEM-100CXII transmission electron microscope (working voltage of 80–100 kV) by the negative-staining method with uranyl acetate solution (1%) as the staining agent. One drop of the solution or a piece of hydrogel was placed onto a carbon Formvar-coated copper grid (230 mesh) for 3~5 min. The excess liquid or hydrogel was sucked away by filter papers. Then one drop of the staining agent was placed onto the copper grid for 2~5 min. The excess staining agent was also sucked away by filter papers.

### Cryogenic transmission electron microscopy (cryo-TEM)

Cryo-TEM samples were prepared in a controlled environment vitrification system (CEVS). A small drop of sample was placed on a copper grid, and a thin film was produced by blotting off the redundant liquid with filter paper. This thin film was then quickly dipped into liquid ethane, which was cooled by liquid nitrogen. The vitrified samples were then stored in liquid nitrogen until they were transferred to a cryogenic sample holder (Gatan 626) and examined by a JEM2200FS TEM (200 kV) at about −174 °C.

### UV-vis absorbance

UV-vis absorbance measurements were carried out on the spectrophotometer (Cary 1E, Varian Australia PTY Ltd.) equipped with a thermostated cell holder. The UV-vis measurement was all carried out at 25 °C.

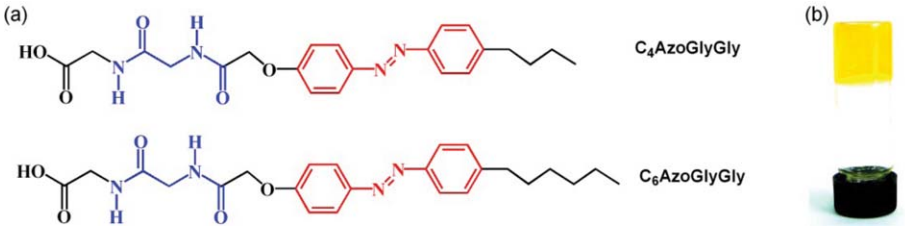


**Fig. 1** (a) Molecular structure of dipeptide-amphiphile $C_4$AzoGlyGly and $C_6$AzoGlyGly; (b) macroscopic appearance of $C_4$AzoGlyGly hydrogel (5 mM).



### Fourier transform IR

The Fourier transform IR spectrum of $C_4$AzoGlyGly solid or hydrogel in $D_2O$ is collected with a Nicolet iN10 MX spectrometer (Thermo Scientific, America).

### Fluorescence measurement

Steady-state fluorescence spectra were obtained with an Edinburgh FLS920 fluorescence spectrophotometer. In these studies, a fixed amount (5.0 μM) of the fluorescent probe Nile Red was added to the aphiphile solution and stirred to reach equilibrium. The excitation wavelength of Nile Red is 575 nm and the fluorescence emission was monitored.

### Circular dichroism (CD)

CD spectra were recorded using a JASCO J-810 spectrometer. The path length of the quartz cell was 0.1 mm and each measurement was repeated three times at 25 °C.

### Photoisomeric experiment

For light-triggered *trans–cis* transition, the samples were irradiated with 365 nm UV light from a Spectroline FC-100F fan-cooled, long wave UV lamp. The power of the mercury arc lamp is 100 W. Samples were placed in a quartz tube, and irradiation was done for a specific duration. For *cis–trans* transition, irradiation by visible light was performed using a 200 W incandescent light bulb (>440 nm). The quartz tube was placed in front of the light source 15 cm away.

## Results and discussion

### Hydrogel formation by dipeptide-amphiphiles

The dipeptide-amphiphile bearing azobenzene and glycylglycine moieties are synthesized as described in the Experimental section (Fig. 1a). $C_4$AzoGlyGly solution is prepared by adding the desired amount of solid into an equal amount of sodium hydroxide solution and heated until completely soluble. After cooling, the sample becomes thicker and can even gelate water. The fluorescence intensity curve of the Nile Red probe indicates the critical aggregates concentration of $C_4$AzoGlyGly solution is about 2 mM (Fig. S1, ESI†). Fig. 1b shows the test-tube inversion of 5 mM $C_4$AzoGlyGly hydrogel in a test tube. The gelation temperature, varied by gelator concentration, is also measured by the test-tube inversion method (Fig. S2, ESI†). To understand the effect of the hydrophobic tail, the dipeptide-amphiphile $C_6$AzoGlyGly (with C6 hydrocarbon chain) is also synthesized. It is found that the lowest gelation concentration (LGC) of $C_6$AzoGlyGly can be lowered to 2 mM while that of $C_4$AzoGlyGly amphiphile is 5 mM.

Dynamic rheology is further performed to investigate the mechanical properties of dipeptide-amphiphile hydrogels. Time sweep rheology in Fig. 2a indicates that a stable hydrogel is quickly formed with 20 mM $C_4$AzoGlyGly in 100 s, in which the storage modulus G′ and the loss modulus G″ can reach a plateau soon after preparation. Nondestructive frequency sweep exhibits typical solidlike rheological behavior with the storage modulus G′ (~60 Pa) dominating the loss modulus G″ (~10 Pa) over the investigated oscillating frequency (Fig. 2b). This is a typical solidlike behavior of a hydrogel.[14] Besides, the storage modulus shows strong dependence on gelator concentration (Fig. S3, ESI†). On the other hand, when the length of the hydrocarbon tail is increased, the hydrogel mechanical intensity can be greatly enhanced (Fig. S4, ESI†). For example, the storage modulus and loss modulus of $C_6$AzoGlyGly is nearly two orders larger than that of $C_4$AzoGlyGly.

### Self-assembled 1D nanostructures from dipeptide amphiphiles

Transmission electronic microscopy (TEM) sampes were prepared by negative-staining technique to reveal the

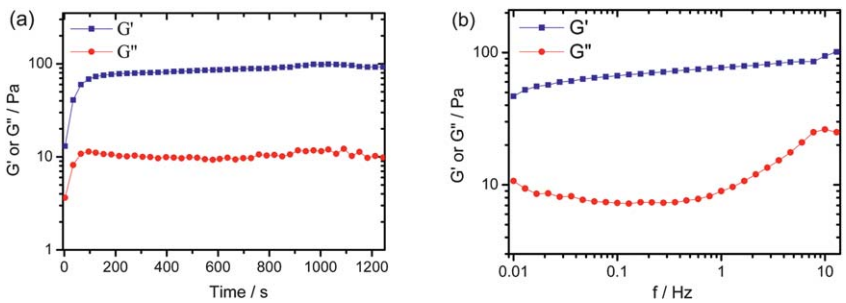


**Fig. 2** Dynamic rheology of self-assembled $C_4$AzoGlyGly hydrogel (C = 20 mM): (a) time sweep; (b) frequency sweep.

 

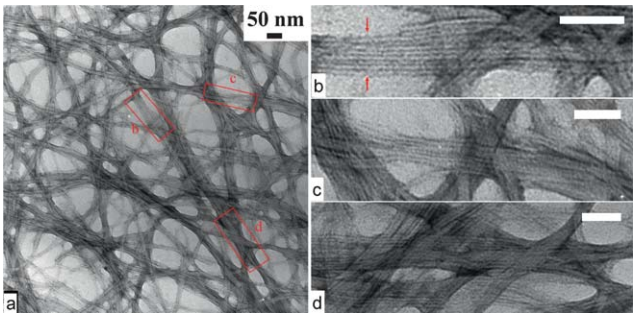


**Fig. 3** Negative-staining TEM images of self-assembled nanostructures in the system of 5 mM $C_4$AzoGlyGly hydrogel.



microstructure of the $C_4$AzoGlyGly hydrogel. As shown in Fig. 3a, the dipeptide-amphiphile $C_4$AzoGlyGly (5 mM) can self-organize into nanoribbons of several micrometres long and tens of nanometres wide. These 1D nanostructures are highly flexible and easy to overlap and entangle with each other, which are responsible for the robustness of hydrogel. The enlarged images (Fig. 3b, 3c and 3) indicate that the nanoribbons are composed of highly ordered lamellar structures with obvious light and shade boundaries. The images show that the ribbons are formed by bundles of parallel nanofibers. The arrows in Fig. 3b indicate a seven-layered nanoribbon with a width of 33 nm. A calculation from the TEM images gives the diameter of a single nanofiber to be 5 nm, which is comparative to double the molecular length of $C_4$AzoGlyGly (~2.5 nm, by MM2 force field simulation). Enlarged images indicate the ribbons are particularly thin so that the overlap patterns of nanoribbons can even be seen from TEM. It is estimated that the thickness of each ribbon is several nanometres which corresponds to a bilayer structure. Even when the amphiphile concentration decreases to 2 mM, the nanoribbons with a laminated structure can be observed (Fig. S5, ESI†).

### Mechanism illustration of molecular self-assembly

Fourier transform infrared (FT-IR) spectroscopy of $C_4$AzoGlyGly in solid state and hydrogel state provides important information about the intermolecular hydrogen bonds among the component molecules (Fig. 4a). The spectrum of the $C_4$AzoGlyGly solid exhibited characteristic absorption bands centered at around 1730 $cm^{-1}$ and 1663 $cm^{-1}$, which is attributed to the amide I band of $C_4$AzoGlyGly solid.[15] In the gel state (in $D_2O$), however, the amide I band of $C_4$AzoGlyGly shifts from 1663 $cm^{-1}$ to 1635 $cm^{-1}$. The 28 $cm^{-1}$ shift of the C=O stretching (1663–1635) may be attributed to further hydrogen bonding involving C=O.[14] The low-frequency amide I bands at 1635 $cm^{-1}$ are characteristic of a $\beta$-sheet configuration. On the other hand, $C_4$AzoGlyGly does not form a $\beta$-sheet structure in the solid state.

To obtain further insight into the submolecular information for the dipeptide-amphiphile self-assembly, circular dichroism (CD) studies are performed (Fig. 4b). When $C_4$AzoGlyGly concentration is 1 mM (below CAC), no notable CD signals are observed. This is in agreement with the TEM result in which self-assembled nanoribbons are not detected. When the $C_4$AzoGlyGly concentration is 2 mM, CD split signals can be noted. The exciton splitting CD bands are observed in the *trans*-azobenzene region (Fig. 4b). A dichroic bands of opposite sign centered at 354 nm are related to the $\pi$–$\pi^*$ transition of the azobenzene chromophore. It is suggested that the dichroic couplet of $C_4$AzoGlyGly in the $\pi$–$\pi^*$ region is the result of exciton splitting owing to dipole–dipole interactions between *trans*-azobenzene disposed in a mutual chiral geometry along the $\beta$-sheet network. The CD signal at low wavelength may be also indicative of $\beta$-sheet formation as suggested by FT-IR.

Combined with these results, we propose a molecular arrangement as well as interpretation for laminated nanoribbons. As shown in Fig. 5a and 5b, the nanoribbons are constructed by the parallel alignment of fibers. The growth of these nanostructures along each dimension is obviously regulated by different forces. It is suggested that one dimensionality is linked to fast growth along the direction of amide hydrogen bonding in $\beta$-sheets (the arrows in Fig. 5c and 5d indicate the H-bond direction). Also the $\pi$–$\pi$ stacking between azobenzene groups will contribute to 1D directional growth of nanofiber. These directional forces (H-bond and $\pi$–$\pi$ stacking) together with nondirectional hydrophobic interaction ultimately promote molecular self-assembly into one-dimensional nanofiber. In the lateral direction, however, hydrogen bond and $\pi$–$\pi$ stacking is lacking. Another question is why the nanofibers will parallel align into ribbons. It is supposed that the carboxyl on the nanofiber surface will be partially hydrolyzed in solution. As a consequence, surface hydrogen bonds will be formed between adjacent fibers which facilitate the affinity and well-alignment of neighboring fibers.

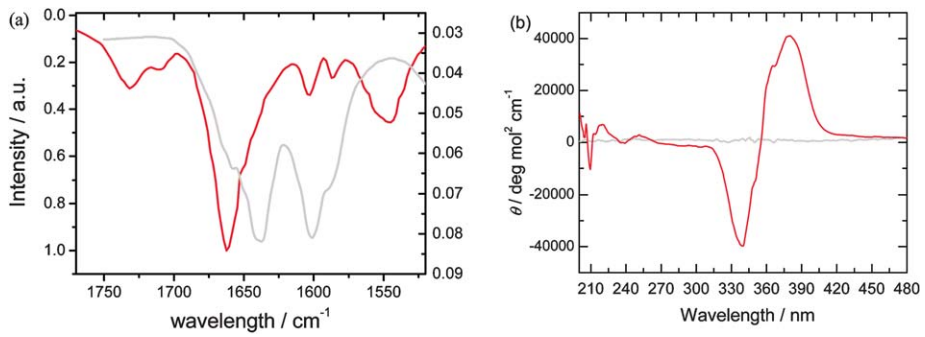


**Fig. 4** (a) FT-IR spectrum of $C_4$AzoGlyGly solid (dark line) and $C_4$AzoGlyGly hydrogel in $D_2O$ (light line). (b) CD spectrum of $C_4$AzoGlyGly solution at 25 °C: 2 mM (dark line) and 1 mM (light line).

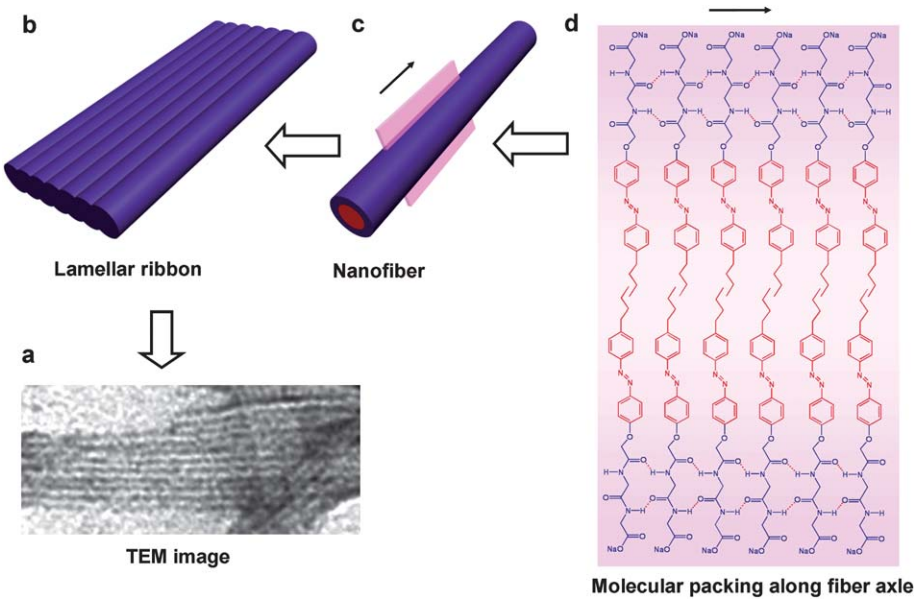


**Fig. 5** Dipeptide-amphiphile self-assembly of $C_4$AzoGlyGly. (a) TEM image; (b) cartoon picture of nanoribbon; (c) an individual fiber; (d) molecular packing in the plane along fiber axis.

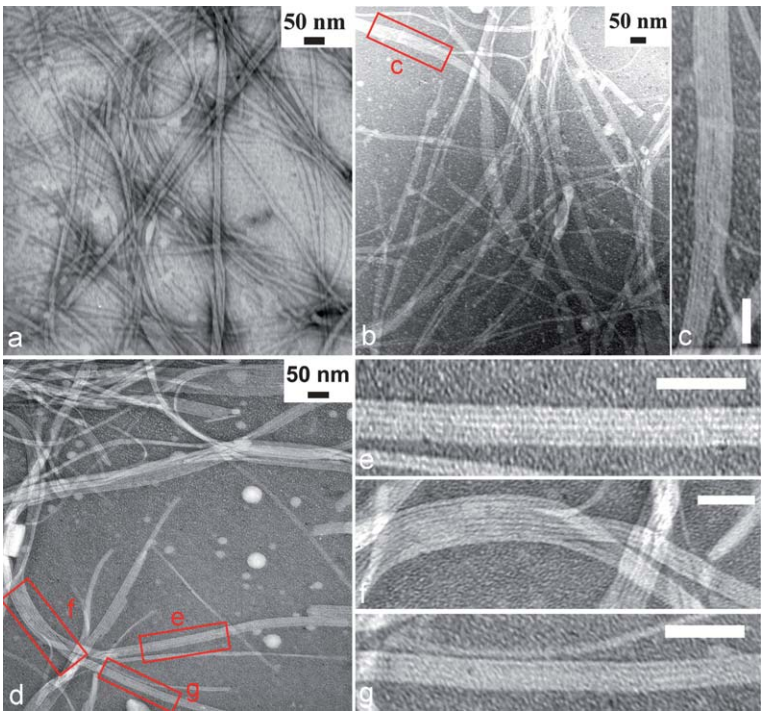


**Fig. 6** TEM images of 1 mM $C_4$AzoGlyGly solution stained with uranyl acetate solution (1%): (a) with 10 mM NaCl; (b, c) with 20 mM NaCl; (d–g) with 40 mM NaCl. The scale bar in these images is 50 nm.

### Salt-promoted water gelation and nanofiber parallel alignment

Considering the electrostatic repulsion between ionic headgroups of $C_4$AzoGlyGly is profound, the addition of inorganic salts are expected to bring remarkable effect towards supramolecular self-assembly. Herein, the self-assembly behavior of dipeptide amphiphile is studied in the absence and presence of NaCl. As demonstrated by TEM, $C_4$AzoGlyGly cannot form aggregates at 1 mM. With addition of 10 mM NaCl, a large amount of one-dimensional nanoribbons can be observed under TEM (Fig. 6a). As NaCl concentration increases to 20 mM or 40 mM, nanoribbons with well-aligned laminated structures become the dominant morphology (Fig. 6b–6g). The CD spectrum shows a notable signal can be detected in $C_4$AzoGlyGly solution (1 mM) with the addition of 20 mM (Fig. 7a). It is suggested that sodium ions can weaken electrostatic repulsion between carboxyl

 

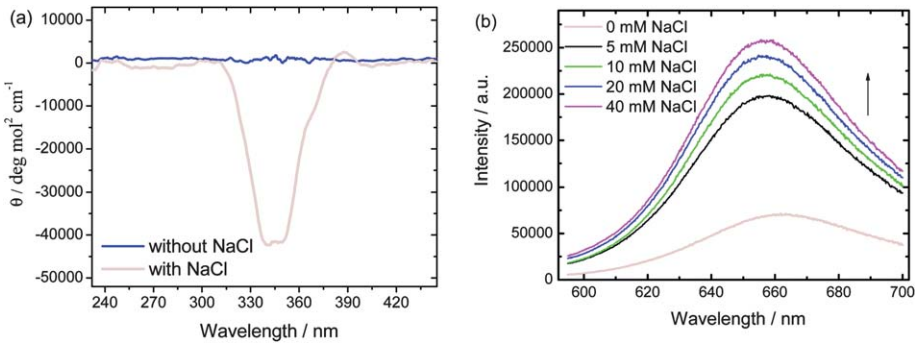


**Fig. 7** (a) CD curve of $C_4$AzoGlyGly (C = 1 mM) solution without NaCl (dark line) or with 20 mM NaCl; (b) Fluorescence intensity of 5 μM Nile Red in $C_4$AzoGlyGly (C = 1.0 mM) solution with the addition of NaCl.

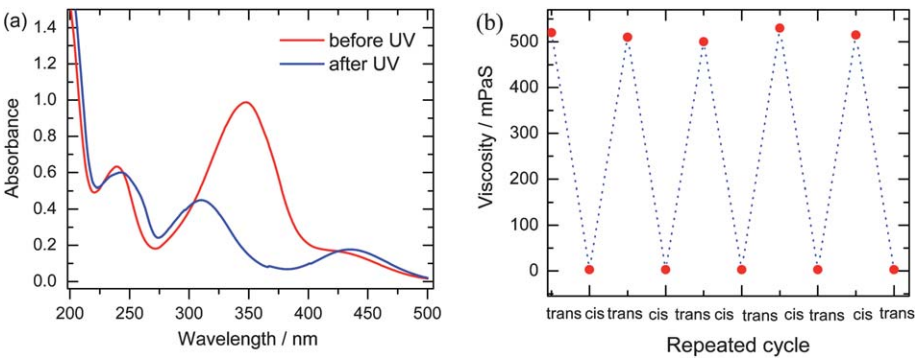


**Fig. 8** (a) UV-vis spectrum of $C_4$AzoGlyGly solution before and after 365 nm light irradiation; (b) Shear viscosity of 5 mM $C_4$AzoGlyGly solution after repeated irradiated by 365 nm UV light and visible light. (The UV irradiation time is 30 min while the visible light irradiation time is 1 h.)



headgroups, which will promote molecular aggregates and facilitate nanofiber alignment into ribbons. This is supported by Nile Red fluorescence intensity as shown in Fig. 7b. Nile Red fluorescence intensity is much greater in hydrophobic environments than in a hydrophilic environment.[16] As shown in Fig. 7b, the fluorescence emission of Nile Red in 1 mM $C_4$AzoGlyGly solution increases gradually with the addition of NaCl. This implies the environment around Nile Red is becoming hydrophobic and the molecular packing inside the aggregates turns to be more closely. In a control experiment, the fluorescence intensity of Nile Red in water does not show an increase with the addition of NaCl (Fig. S6, ESI†).

### Light-triggered supramolecular self-assembly

The incorporation of azobenzene group can impart light-active behavior to the self-assembled $C_4$AzoGlyGly solution. As shown in Fig. 8a, before UV light irradiation, the spectrum is dominated by the 349 nm absorption which is ascribed to the π–π* absorption band of the *trans*-azobenzene moiety. As UV irradiation proceeds, the 349 nm absorption band decreases with concomitant increase of the π–π* and n–π* bands of the *cis* isomer at around 310 nm and 440 nm, respectively. The UV-vis result strongly demonstrates the azobenzene *trans–cis* transition triggered by UV or visible light. Meanwhile, such a conformational change can be reversibly repeated by light.

Rheological measurements show a dramatic viscosity decrease after exposing to UV light. When visible light is applied, the viscosity can be reverted and the sample turns into highly viscous hydrogel (Fig. 8b). It is believed that the variation of flowing property at the macroscale originates from the structural evolution at the nanoscale. The TEM images show that the nanoribbon networks in 5 mM $C_4$AzoGlyGly hydrogels have transformed into short fibers after 30 min UV light irradiation (Fig. 9a). Cryo-TEM results also demonstrate the formation of a small amount of short fibers in 5 mM $C_4$AzoGlyGly solution after UV irradiation (Fig. 9b). It is worthwhile that laminated nanoribbons can be re-formed after irradiation by visible light (Fig. S7, ESI†). Fig. 10a shows the light-triggered *trans–cis* transition causes the disappearance of the CD signal after UV light illumination. Meanwhile, the fluorescence intensity of Nile Red in $C_4$AzoGlyGly solution decreases sharply after UV irradiation (Fig. 10b), implying molecular packing inside the aggregates becomes more loose.

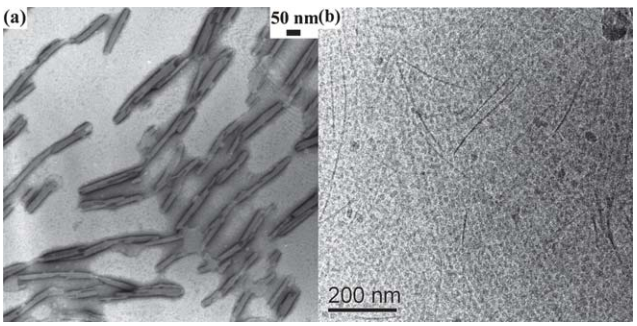


**Fig. 9** (a) Negative-staining TEM and (b) cryo-TEM images of a 5 mM $C_4$AzoGlyGly sample illuminated by UV light for 30 min.

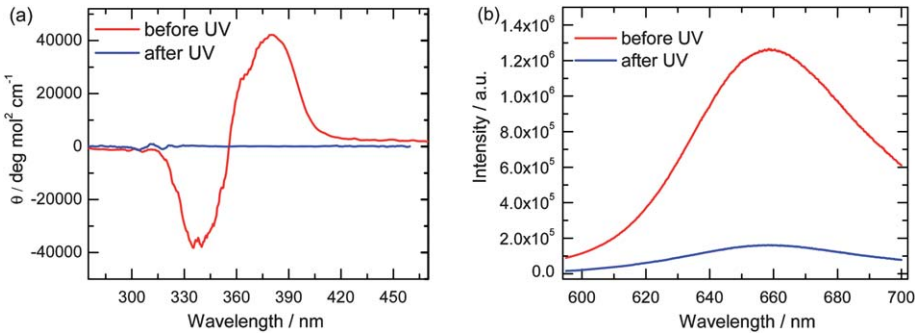


**Fig. 10** (a) CD spectrum of $C_4$AzoGlyGly solution before and after 365 nm light irradiation; (b) Fluorescence intensity of Nile Red in $C_4$AzoGlyGly solution (5 mM) before and after 365 nm light irradiation. (The UV irradiation time is 30 min while the visible light irradiation time is 1 h.)



It is acknowledged that azobenzene can undergo photo-induced isomerism accompanied by large structural change as reflected in the dipole moment and change in geometry.[17] On one hand, the planar *tran*-azobenzene group transforms into nonplanar *cis*-azobenzene and the aromatic packing between azobenzene groups is suppressed. On the other hand, *trans*-azobenzene has no dipole moment while the dipole moment of the *cis*-azobenzene is 3.0 D. In other words, *cis*-azobenzene is more hydrophilic than *trans*-azobenzene. Owing to the weakening of π–π stacking (directional) and hydrophobic effect (nondirectional), elongated nanostructures are not favored in *cis*-$C_4$AzoGlyGly solution. Meanwhile, the decrease of π–π stacking between azobenzene groups ultimately weakens the CD signal.

## Conclusion

In conclusion, novel dipeptide derivatives bearing azobenzene group are synthesized which can spontaneously self-assemble into well-defined nanoribbons as well as sample-spanning networks forming hydrogels in water. The nanoribbons are found to be fabricated by the alignment of nanofibers parallel to the fiber's long axis. The driving force for self-organized nanostructures is believed to come from directional forces (hydrogen bonding and aromatic packing) and the nondirectional hydrophobic effect. Inorganic salt is demonstrated to suppress the electrostatic repulsion and favor the nanoribbon formation. Furthermore, laminated nanoribbons can transform into short fibers under UV irradiation, which revert to nanoribbons by visible light exposure. It is expected that this work can shed light on stimuli-responsive molecular self-assembly and the rational design of hierarchical nanostructures through a bottom-up approach.

## Acknowledgements

This work is supported by National Natural Science Foundation of China (20873001, 20633010, 50821061 and 21073006) and National Basic Research Program of China (Grant No. 2007CB936201).

## References

1 J. M. Schnur, B. R. Ratna, J. V. Selinger, A. Singh, G. Jyothi and K. R. K. Easwaran, *Science*, 1994, **264**, 945; J. M. Schnur, *Science*, 1993, **262**, 1669; E. Winfree, F. Liu, L. A. Wenzler and N. C. Seeman, *Nature*, 1998, **394**, 539; H. Yan, S. H. Park, G. Finkelstein, J. H. Reif and T. H. LaBean, *Science*, 2003, **301**, 1882; F. F. Miranda, K. Iwasaki, S. Akashi, K. Sumitomo, M. Kobayashi, I. Yamashita, J. R. H. Tame and J. G. Heddle, *Small*, 2009, **5**, 2077; B. N. Thomas, R. C. Corcoran, C. L. Cotant, C. M. Lindemann, J. E. Kirsch and P. J. Persichini, *J. Am. Chem. Soc.*, 1998, **120**, 12178; S. G. Zhang, *Nat. Biotechnol.*, 2003, **21**, 1171; B. H. Ozer, B. Smarsly, M. Antoniettia and C. F. J. Faul, *Soft Matter*, 2006, **2**, 329.
2 D. M. Fowler, A. V. Koulov, W. E. Balch and J. W. Kelly, *Trends Biochem. Sci.*, 2007, **32**, 217; A. C. Clark and S. B. Ross-Murphy, *Adv. Polym. Sci.*, 1987, **83**, 57; *The Science and Technology of Gelatin*, ed. A. G. Ward and T. A. Courts, Academic Press, London, 1977; *Biorelated Polymers and Gels*, ed. T. Okano, Academic Press, San Diego 1998; W. Shen, J. A. Kornfield and D. A. Tirrell, *Soft Matter*, 2007, **3**, 99.
3 R. Fairman and K. S. Akerfeldt, *Curr. Opin. Struct. Biol.*, 2005, **15**, 453; S. G. Zhang, T. Holmes, C. Lockshin and A. Rich, *Proc. Natl. Acad. Sci. U. S. A.*, 1993, **90**, 3334; S. Vauthey, S. Santoso, H. Y. Gong, N. Watson and S. G. Zhang, *Proc. Natl. Acad. Sci. U. S. A.*, 2002, **99**, 5355; T. J. Deming, *Nature*, 1997, **390**, 386; T. J. Deming, *Soft Matter*, 2005, **1**, 28; J. P. Schneider, D. J. Pochan, B. Ozbas, K. Rajagopal, L. Pakstis and J. Kretsinger, *J. Am. Chem. Soc.*, 2002, **124**, 15030; R. P. Nagarkar, R. A. Hule, D. J. Pochan and J. P. Schneider, *J. Am. Chem. Soc.*, 2008, **130**, 4466; A. Aggeli, I. A. Nyrkova, M. Bell, R. Harding, L. Carrick, T. C. B. McLeish, A. N. Semenov and N. Boden, *Proc. Natl. Acad. Sci. U. S. A.*, 2001, **98**, 11857; R. J. Mart, R. D. Osborne, M. M. Stevens and R. V. Ulijn, *Soft Matter*, 2006, **2**, 822; I. W. Hamley, M. J. Krysmann, A. Kelarakis, V. Castelletto, L. Noirez, R. A. Hule and D. J. Pochan, *Chem.–Eur. J.*, 2008, **14**, 11369; A. J. Dirks, S. S. van Berkel, H. I. V. Amatdjais-Groenen, F. P. J. T. Rutjes, J. J. L. M. Cornelissen and R. J. M. Nolte, *Soft Matter*, 2009, **5**, 1692.
4 C.-L. Chen and N. L. Rosi, *Angew. Chem. Int. Ed.*, 2010, **49**, 1924; M. P. Lutolf and J. A. Hubbell, *Nat. Biotechnol.*, 2005, **23**, 47; J. N. Cha, G. D. Stucky, D. E. Morse and T. J. Deming, *Nature*, 2000, **403**, 289.
5 H.-W. Jun, S. E. Paramonov and J. D. Hartgerink, *Soft Matter*, 2006, **2**, 177; S. Toledano, R. J. Williams, V. Jayawarna and R. V. Ulijn, *J. Am. Chem. Soc.*, 2006, **128**, 1070; R. V. Ulijn, *J. Mater. Chem.*, 2006, **16**, 2217; Y. Zhang, H. Gu, Z. Yang and B. Xu, *J. Am. Chem. Soc.*, 2003, **125**, 13680; Z. Yang, H. Gu, D. Fu, P. Gao, J. K. Lam and B. Xu, *Adv. Mater.*, 2004, **16**, 1440; Y. Matsuzawa, K. Ueki, M. Yoshida, N. Tamaoki, T. Nakamura, H. Sakai and M. Abe, *Adv. Funct. Mater.*, 2007, **17**, 1507; M. L. Deng, D. F. Yu, Y. B. Hou and Y. L. Wang, *J. Phys. Chem. B*, 2009, **113**, 8539; X. H. Yan, Q. He, K. W. Wang, L. Duan, Y. Cui and J. B. Li, *Angew. Chem., Int. Ed.*, 2007, **46**, 2431; Y.-R. Yoon, Y.-B. Lim, E. Lee and M. Lee, *Chem. Commun.*, 2008, 1892; D. J. Adams and P. D. Topham, *Soft Matter*, 2010, **6**, 3707.
6 J. D. Hartgerink, E. Beniash and S. I. Stupp, *Science*, 2001, **294**, 1684.
7 J. D. Hartgerink, E. Beniash and S. I. Stupp, *Proc. Natl. Acad. Sci. U. S. A.*, 2002, **99**, 5133; R. C. Claussen, B. M. Rabatic and S. I. Stupp, *J. Am. Chem. Soc.*, 2003, **125**, 12680; K. L. Niece, J. D. Hartgerink,

 

J. J. J. M. Donners and S. I. Stupp, *J. Am. Chem. Soc.*, 2003, **125**, 7146; A. Mata, L. Hsu, R. Capito, C. Aparicio, K. Henriksonc and S. I. Stupp, *Soft Matter*, 2009, **5**, 1228.
8 H. Dong, S. E. Paramonov, L. Aulisa, E. L. Bakota and J. D. Hartgerink, *J. Am. Chem. Soc.*, 2007, **129**, 12468; V. Gauba and J. D. Hartgerink, *J. Am. Chem. Soc.*, 2007, **129**, 2683.
9 T. Shimizu, M. Kogiso and M. Masuda, *J. Am. Chem. Soc.*, 1997, **119**, 6209; T. Shimizu, M. Kogiso and M. Masuda, *Nature*, 1996, **383**, 487.
10 N. Kameta, H. Minamikawa, M. Masuda, G. Mizunoc and T. Shimizu, *Soft Matter*, 2008, **4**, 1681; H. Matsui, S. Pan, B. Gologan and S. H. Jonas, *J. Phys. Chem. B*, 2000, **104**, 9576; R. Djalali, Y.-F. Chen and H. Matsui, *J. Am. Chem. Soc.*, 2003, **125**, 5873; R. V. Ulijn and A. M. Smith, *Chem. Soc. Rev.*, 2008, **37**, 664; D. Khatua, R. Maitib and J. Dey, *Chem. Commun.*, 2006, 4903; H. M. Wang, C. H. Ren, Z. J. Song, L. Wang, X. M. Chen and Z. M. Yang, *Nanotechnology*, 2010, **21**, 225606; Y. H. Hu, H. M. Wang, J. Y. Wang, S. B. Wang, W. Liao, Y. G. Yang, Y. J. Zhang, D. L. Kong and Z. M. Yang, *Org. Biomol. Chem.*, 2010, **8**, 3267; J. Gao, H. M. Wang, L. Wang, J. Y. Wang, D. L. Kong and Z. M. Yang, *J. Am. Chem. Soc.*, 2009, **131**, 11286; Z. J. Qiu, H. T. Yu, J. B. Li, Y. Wang and Y. Zhang, *Chem. Commun.*, 2009, 3342.
11 H. Sakai, A. Matsumura, S. Yokoyama, T. Saji and M. Abe, *J. Phys. Chem. B*, 1999, **103**, 10737; A. M. Ketner, R. Kumar, T. S. Davies, P. W. Elder and R. S. Raghavan, *J. Am. Chem. Soc.*, 2007, **129**, 1553; J. Eastoe, A. H. Zou, Y. Espidel, O. Glatter and I. Grillo, *Soft Matter*, 2008, **4**, 1215.
12 Y. Y. Lin, A. D. Wang, Y. Qiao, C. Gao, M. Drechsler, J. P. Ye, Y. Yan and J. B. Huang, *Soft Matter*, 2010, **6**, 2031.
13 X. D. Song, J. Perlstein and D. G. Whitten, *J. Am. Chem. Soc.*, 1997, **119**, 9144.
14 *Molecular Gels: Materials with Self Assembled Fibrillar Network*; Weiss, R. G., Terech, P., ed.; Spinger: Dordrecht, 2006.
15 D. K. Kumar, D. A. Jose, P. Dastidar and A. Das, *Langmuir*, 2004, **20**, 10413.
16 B. A. Cicciarelli, T. A. Hatton and K. A. Smith, *Langmuir*, 2007, **23**, 4753; D. L. Sackett and J. Wolff, *Anal. Biochem.*, 1987, **167**, 228; M. C. A. Stuart, J. C. van de Pas and J. B. F. N. Engberts, *J. Phys. Org. Chem.*, 2005, **18**, 929.
17 G. S. Kumar and D. C. Neckers, *Chem. Rev.*, 1989, **89**, 1915; C. Dugave and L. Demange, *Chem. Rev.*, 2003, **103**, 2475; T. Hayashita, T. Kurosawa, T. Miyata, K. Tanaka and M. Igawa, *Colloid Polym. Sci.*, 1994, **272**, 1611; C. T. Lee, K. A. Smith and T. A. Hatton, *Macromolecules*, 2004, **37**, 5397; Y. P. Wang, N. Ma, Z. Q. Wang and X. Zhang, *Angew. Chem., Int. Ed.*, 2007, **46**, 2823.